

# The Influence of Injection pressure on Combustion and Emission Characteristics of a common-rail HSDI Diesel Engine

Hayder A.Dhahad<sup>1</sup>, Mohammed A. Abdulhadi<sup>1</sup>, Ekhlash M.Alfayydh<sup>1</sup>, T. Megaritis<sup>2</sup>

<sup>1</sup> University of technology – Baghdad –Iraq

<sup>2</sup> Brunel University, UK

## Abstract

The present work investigates the influence of fuel injection pressure on the combustion and emission characteristics of ultra-low diesel fuel for high speed direct injection (HSDI) diesel engine at different fuel injection timings ( -12,-9,-6,-3,0 )ATDC has been made . The fuel injection pressure were (800,1000,1200) bar and at high load ( 80Nm= 5BMAP ) , low load ( 40Nm=2.5BMAP ) , With constant engine speed ( 1500rpm ) . In-cylinder pressure was measured and analyzed using LABVIWE program .A calculation program specially written in MATLAB software was used to extract the apparent heat release rate, the ignition delay, combustion duration and specifies the amount of heat released during the premixed and diffusion combustion phases ( premixed burn fraction PMBF) and ( diffusion burn fraction DBF). The influence of injection pressure on the exhaust emissions such as carbon monoxide (CO), total hydrocarbons (THCs), nitric oxides (NO<sub>x</sub>), smoke number (SN) and fuel consumption were also investigated.

A result referring to that when the injection pressure was increased, the ignition delay reduced. A shorter ignition delay at high injection pressure also advanced the combustion, and increased the in-cylinder pressure, heat release rate and their peaks respectively .The premixed burn fraction increased with fuel injection pressure increasing, and this caused a decrease in each of the exhaust SN, THC and CO emissions but the NO<sub>x</sub> emissions increased.

Key words: combustion, diesel engine, injection pressure, gases emissions.

## المخلص

هذا البحث درس تأثير ضغط الحقن على خصائص الاحتراق والانبعاثات لوقود الديزل منخفض الكبريت باستخدام محرك ديزل عالي السرعة وذو حقن مباشر ومع تغيير توقيت الحقن عند ( -12,-9,-6,-3,0 )ATDC , ضغط الحقن للوقود كان ( 800,1000,1200 ) ضغط جوي واجريت التجارب عند الحمل العالي ( 80Nm= 5BMAP ) والحمل المنخفض ( 40Nm=2.5BMAP ) , تم تثبيت سرعة المحرك عند 1500 rpm . تم قياس الضغط داخل غرفة الاحتراق ومن ثم تحليل الضغط باستخدام برنامج LABVIWE وبرنامج حسابي باستخدام برنامج MATLAB لحساب معدل الحرارة المنطلقة و تاخر الاشتعال و مدة الاحتراق وكمية الحرارة المنطلقة في طور الاحتراق المسبق الخلط وكذلك في طور الاحتراق الانتشاري . تأثير ضغط الحقن على انبعاثات غازات العادم مثل اول اوكسيد الكربون (CO) الهادروكربون غير المحترق الكلي (THC) واكاسيد الناتروجين (NO<sub>x</sub>) ورقم الدخان (SN) ومعدل استهلاك . النتائج اشارة الى ان زيادة ضغط الحقن نتج عنه نقصان في تاخر الاشتعال وبالتالي تقدم في بداية الاحتراق وزيادة ضغط الاسطوانة ومعدل الحرارة المنطلقة ،ان زيادة جزء الاحتراق المسبق الخلط عند زيادة ضغط الحقن سبب نقصان في انبعاثات العادم لكل من SN و THC و CO ولكن انبعاث NO<sub>x</sub> يزداد.

## NOMENCLATURE

AHRR	Apparent heat release rate
ATDC	After top dead centre
BMAP	Brake mean effective pressure
CI	Compression ignition
CO	Carbon monoxide
CO <sub>2</sub>	Carbon dioxide
C <sub>p</sub>	Specific heat at constant pressure
C <sub>v</sub>	Specific heat at constant volume
DBF	Diffusion burn fraction
EGR	Exhaust Gas Recirculation
EOC	End of combustion
EOPMB	End of premixed burn
HCCI	Homogenous Charge Compression Ignition
HSDI	High speed direct injection
ID	Ignition delay
LTC	Low Temperature Combustion
NO	Nitrogen monoxide
NO <sub>2</sub>	Nitrogen dioxide
NO <sub>x</sub>	Nitric oxides
PCCI	Premixed Charge Compression
PM	Particulate matter
PMBF	Premixed burn fraction
SOC	Start of combustion
SOI	Start of injection
Sox	Sulfur oxides
SN	Smoke number
THCs	Total hydrocarbons
ULSD	Ultra-low sulfur diesel fuel

### 1. Introduction

Although the advantages of high thermal efficiency and high performance of the compression ignition (CI) engine, the unburned or partially burned (total) hydrocarbon (THC) emissions, smoke (soot) or particulate matter (PM), nitrogen oxides (NO<sub>x</sub>), sulfur oxides (SO<sub>x</sub>) emitted from compression ignition (CI) engines and particularly carbon dioxide (CO<sub>2</sub>) create severe environmental problems (Shah et al2009, Abdel-Rahman 1998 , Lebedevas and Vaicekaskas 2006 ). The past two decades have witnessed drastic reductions in regulated limits for pollutant emissions from diesel engines. For example, heavy-duty engine emissions limits in the United States ( EPA 2003) , the European Union ( EEC1998,EEC1999, EPC 2009) , and Japan (DieselNet 2009) for particulate matter (PM), nitrogen oxides (NO<sub>x</sub>) and unburned hydrocarbons (THC) in the early 2010s are only 2%,  $3 \cdot 10^{-12}$ %, and  $6 \cdot 10^{-12}$ %, respectively, of their 1990 levels. Comparable reductions were also required in the light duty sector (DieselNet 2009, EPA2010). Likewise, in China and India, the evolution of emissions regulations for both

heavy- and light-duty diesel engines from 2000 through 2010 required reductions of similar magnitudes, mirroring the Euro I through Euro IV regulatory limits, though at an accelerated pace (DieselNet 2009) .

Soot formation has been extensively investigated with regard to combustion characteristics (Suzuk et al 1997 Part 1, Suzuk et al 1997 Part 2, Senda et al1999, Kawano et al 2001, Adomeit et al 2006) and application of alternative fuels (Miyamoto et al1998, Kitamura et al 2001, Xu and Lee 2006). The model of soot formation in diesel spray has been proposed by Dec (Dec 1997) and it is illustrated in Figure (1)

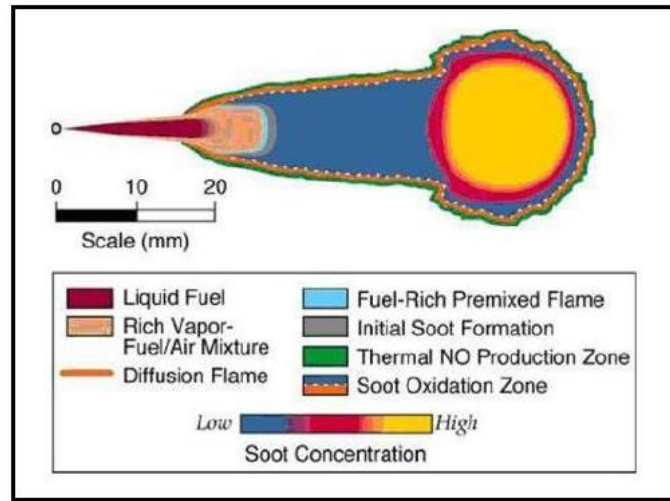


Figure (1) Conceptual model of the soot formation process in diesel spray, proposed by (Dec 1997)

This model predicts that primary soot particles initially form at the leading edge of the liquid fuel jet where rich premixed combustion takes place due to initial fuel mixing process. However, as the vapor jet progresses across the cylinder, secondary soot particles, accountable for the majority of soot emissions produced by diesel engines, form downstream of the jet particularly around the jet periphery whereby mixing controlled diffusion combustion occurs. Other major pollutants formed during diesel combustion are nitrogen oxides, commonly referred to as NO<sub>x</sub>. The oxides of nitrogen present in the diesel exhaust gas consist of approximately 70-90% Nitrogen Monoxide (NO) and 10-30% Nitrogen Dioxide (NO<sub>2</sub>) (Majewski and Khair 2006) . nearly all NO<sub>x</sub> emission is formed between the start of combustion and the first 20° of crank angle. Therefore most NO<sub>x</sub> reducing techniques are focused on this critical period (Challen and Baranescu 1999) . one of the major difficulties in conventional diesel engines is the NO<sub>x</sub>-soot trade off. Premixed combustion, during which in-cylinder pressure and temperature are very high, plays an important role in NO formation (Peirce et al 2013). Techniques to control NO<sub>x</sub> formation are mainly linked to a reduction in combustion temperature during this phase of combustion. Unfortunately, a reduction in combustion temperature also leads to an increase in PM emissions. new and renewable fuels are being used for a possible

effective replacement of the conventional diesel fuel either partially or completely (Labecki and Ganippa2012) .Furthermore ,diverse combustion and injection strategies (Low Temperature Combustion LTC, Homogenous Charge Compression Ignition HCCI, Premixed Charge Compression PCCI) have been studied among many research groups to reduce the exhaust emission and simultaneously increase the thermal efficiency of engine (Rakesh et al2013, Kokjohn and Reitz2010, Li et al 2010, Zhen Huang et al2013).The introduction of the common rail fuel injection system in the 1990s allowed greater control over the fuel injection rate and timing over the entire operating range of diesel engines. The fuel injection pressure is independent of the engine speed; thus, capable of promoting improved fuel evaporation and mixture formation at low speeds and loads. Such control over fuel injection system resulted in the development of alternative injection strategies through the application of split or multiple injections aimed at reduction of exhaust emissions while maintaining good level of fuel economy and combustion efficiency. Recent studies on NO<sub>x</sub> and soot formation involved detailed analysis of the effect of alternative fuels (Kwanhee et al 2013, Sara Pinzi et al 2013, Karavalakis et al2010, Kawano et al2010, Kim et al2013, Ushakov et al 2013, Bermudez et al 2011, Kegl 2011), fuel injection timing (Seung et al 2011, Mani and Nagarajan 2009 ), injection strategy (Díez et al2012, Herfatmanesh and Hua Zhao2013) , and Exhaust Gas Recirculation (EGR) (Desantes et al 2013, Bermúdez et al2011, Sarangi et al2010) , fuel injection pressure (Rakopoulos2012, Manasra and Brueggemann2011, Sayin and Gumus 2011, Puhan et al 2009). Modifications of engine operating parameters through the application of the aforementioned techniques resulted in significant reduction in soot emission. The present work investigates the effect of fuel injection pressure to understand the combustion and emission characteristics of ultra-low sulfur diesel fuel (ULSD) in a high speed direct injection diesel engine HSDI and that use of the modern fuel injection system type common rail injection system.

## **2- METHODOLOGY**

### **2-1- Experimental setup and test conditions**

Experiments were carried out in a 2 liter, 4 cylinders, 16 valves, compression ratio18.2, direct Injection Ford diesel engine, coupled to a Schenck eddy current dynamometer. The schematic of the experimental setup is shown in [figure \(2\)](#).

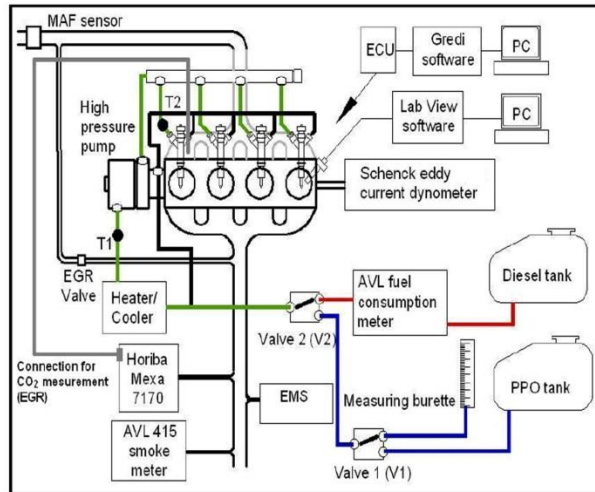


Figure 2. The schematic of experimental setup

In this investigation the engine was operated under naturally aspirated mode. The engine is fully instrumented, which enables the measurement of in-cylinder pressure and exhaust gas emissions under steady-state engine operating conditions. The in-cylinder pressures were measured using a Kistler pressure transducer fitted into the first cylinder of the engine. The signal from pressure transducer was amplified by the charge amplifier and then recorded by the LabView software in conjunction with the shaft encoder. In-cylinder pressure data were collected over 100 engine cycles per measurement, and the measurement was repeated 5 times for each point in the experimental matrix. The in-cylinder pressure data was averaged from 100 cycles. Output from the LabVIEW program are showed in figure (3).

A common rail fuel injection system with six holes injector of 0.154 mm in diameter each, and a spray-hole angle of 154 degree was used in this investigation. In this study, the influence of injection timing has been tested. The Gredi software allowed the control and change of these parameters by programming the ECU in real time. Injection timing could be directly controlled through the software. The gaseous exhaust emissions were acquired using a Horiba-Mexa 7170DEGR gas analyser. A non-dispersive infrared method has been used for measuring the CO and CO<sub>2</sub> emissions. The NO<sub>x</sub> emissions have been measured using chemiluminescence technique whereas the total unburnt hydrocarbons (THC) were measured using the flame ionization detection technique, figure (4) shows a sample of these measurements.

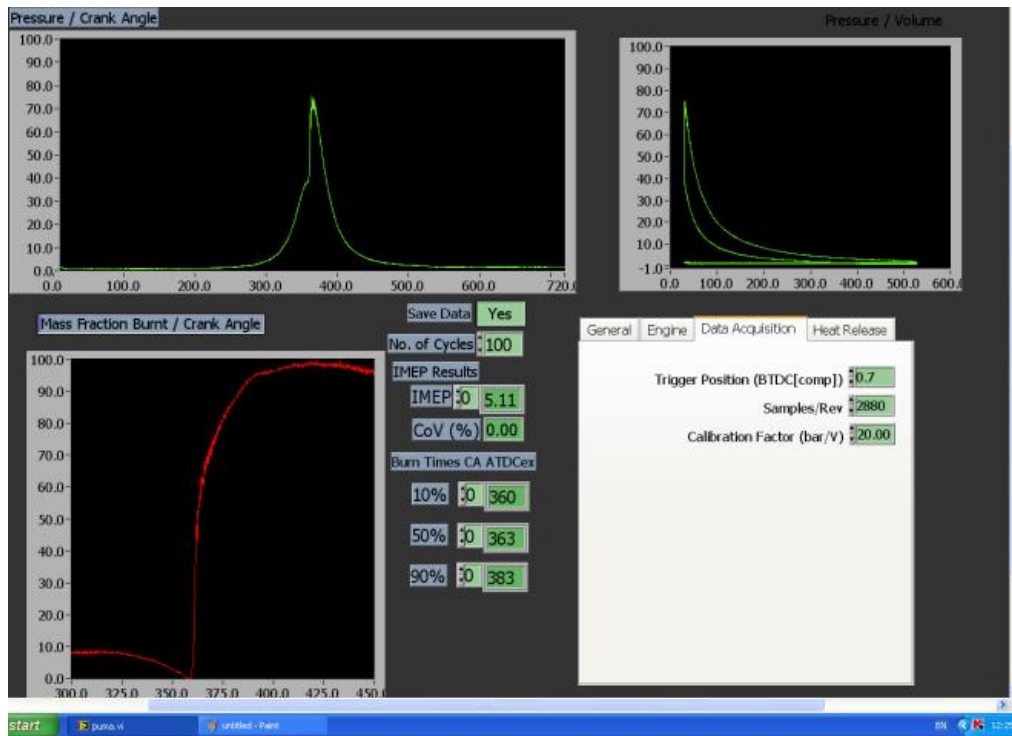


Figure (3) LabVIEW program screen

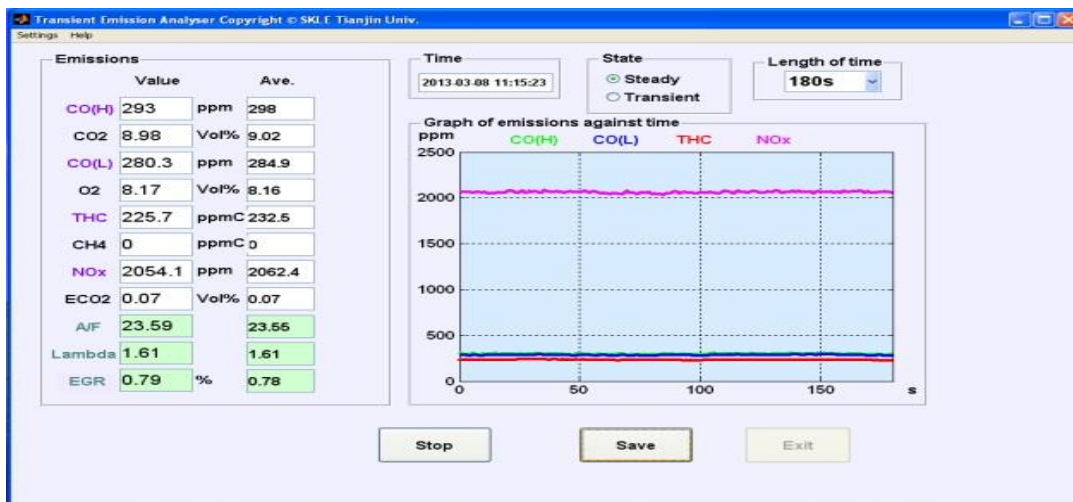


Figure (4) Horiba measurement screen

Emissions data were recorded over 180 seconds intervals, twice for each point in the experimental matrix. Again, this process was repeated for confirmatory purposes. The engine exhaust smoke emissions were measured using the AVL – 415 smoke meter while the diesel fuel consumption was measured using an AVL fuel consumption meter, which is based on gravimetric measurement principle .

Measurements were carried out using the standard ultra-low sulfur diesel fuel. Table (1) provides an overview of all tested engine operating conditions. The load and speed conditions have been chosen to represent the commonly used operating condition for the stationary driving cycle for automotive diesel engines.

Table (1) experiment matrix

Load	Engine Speed rpm	Injection pressure (bar)	Injection timing ATDC
40 nm = 2.5 bar (BMEP)	1500	800	-12
			-9
			-6
			-3
			0
		1000	-12
			-9
			-6
			-3
			0
80 nm =5 bar (BMEP)	1500	1000	-12
			-9
			-6
			-3
			0
		1200	-12
			-9
			-6
			-3
			0

After start-up, the engine was allowed to warm up until hydrocarbon emissions (the slowest pollutant to stabilize) had settled to an apparent steady state; this typically took around 90 min under an 80 Nm load. At each operational condition data collection was postponed until all emissions had reached apparent consistency when viewed over a 180 seconds duration.

## 2-2 Data Analysis

Raw data collected using LabView was loaded into MATLAB and batch processed to retrieve the pertinent information. In-cylinder pressure was processed to extract relevant data-peak pressure, angle of peak pressure, angle between start of combustion (SOC) and peak pressure- and to calculate apparent heat release rate (AHRR) data using the traditional first law heat release model (Heywood 1988) without any modeling of heat transfer or crevice effects, and using an assumed constant specific heat ratio of 1.35. This is a very basic approach, but it is held to be sufficient for the purposes of comparison.

Approximations of  $c_p/c_v$  were made from the logarithm of pressure versus logarithm of volume charts in order to ensure that a constant value would represent fuel equally well. The calculated ratios of specific heats were found to be essentially consistent for ULSD under varying conditions, and so an assumed value of 1.35 was found to be adequate.

The definitions on which calculations of AHRR related parameters were based are illustrated in Figure (5) and explained in the accompanying text. Each 100 cycle pressure data set was used to generate a single average pressure trace, in order to reduce noise while maintaining the essential characteristics of combustion. It should also be noted that

although pressure data was only logged by the data acquisition system once per crank angle degree, all values were interpolated to one decimal place by the MATLAB code. All heat release parameters were calculated from the AHRR curve without filtering or averaging, except for the end of combustion, which was defined on the basis of the moving average of AHRR in order to improve consistency, and the end of premixed burn, which was calculated from the second derivative of AHRR. The following is a definition of the combustion characteristics in the figure (5).

1. Start of injection (SOI) was defined from the commanded SOI set within the engine management software. Any potential difference between commanded and actual SOI, due to solenoid delay for instance, should be consistent between measurements, since engine speed was held constant.
2. Ignition delay (ID) was defined as the difference between commanded SOI and calculated SOC.
3. Start of combustion (SOC) was defined as the point at which the AHRR curve crossed the x axis; that is, the heat release rate became positive.
4. Premixed burn fraction (PMBF) was defined as the integral of the AHRR curve between SOC and EOPMB, divided by the integral of the AHRR curve between SOC and EOC.
5. End of premixed burn (EOPMB) was defined as the first point at which the second differential of heat release rate reached a local maximum following the global minimum. Under most conditions, this approximately corresponds to the position at which the AHRR reaches a first local minimum following the global maximum, but the second differential was used instead because under low loads there local minimum in the AHRR curve is not always clear, as can be seen in Figure 5.
6. End of combustion (EOC) was defined as the first point at which the moving average of heat release rate dropped below zero. A moving average was used to minimize problems due to noise, while still being representative of the general tendencies of the data.

Other values calculated from the in-cylinder pressure data including total apparent heat release, peak AHRR, PMBF, 10–90% burn fraction intervals, duration of partial burn fraction intervals, and average burn rates through partial intervals. Emissions data were averaged over the 180 s durations recorded.

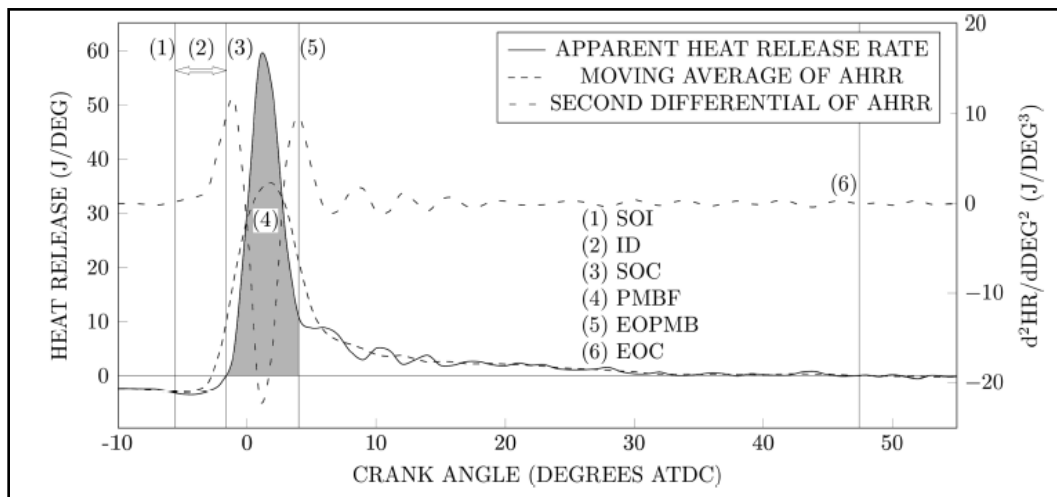


Fig.( 5 ) Labeled plot of heat release and the derivatives used to calculate combustion criteria

### 3-Results and discussions

#### 3-1 Combustion characteristics

Figure (6) shows the variations of the in-cylinder pressure with crank angle at high load ( 80 N.m= 5 bar BMEP ) with variation of fuel injection pressure at injection timing ( -9 ATDC ), it can be seen that as the fuel injection pressure increases from 800 bar to 1200 bar the combustion starts earlier. In addition to this, the in-cylinder pressure peak increases with higher fuel injection pressure. we also note the shift in the location of pressure peaks. The rise in the momentum of the fuel spray leads to better entrainment of air into the core of the fuel spray. In addition to this, high injection pressure provides more energy to break up higher viscous fuels into smaller droplets, leading to faster evaporation at the periphery of the fuel sprays and faster ignition of the fuel vapour.

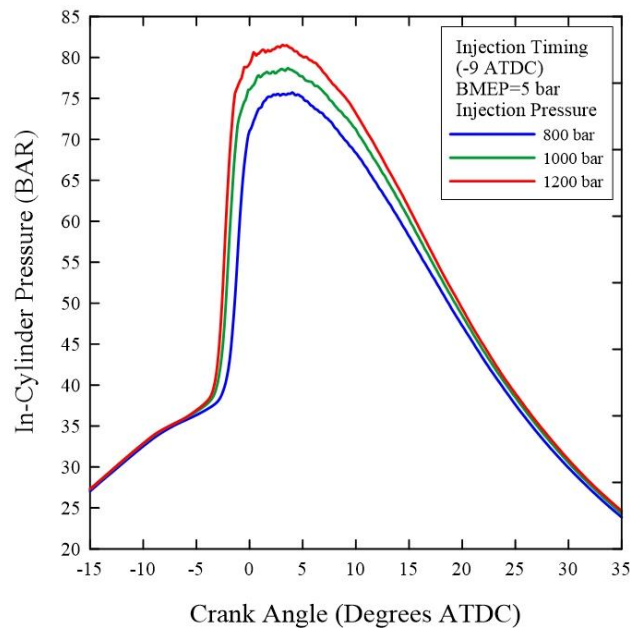


Figure (6) In-cylinder pressure under 80Nm (5 bar BMEP) at different injection pressure

The same events occurs at the low load (40 N.m= 2.5 bar BMEP) figure (7).

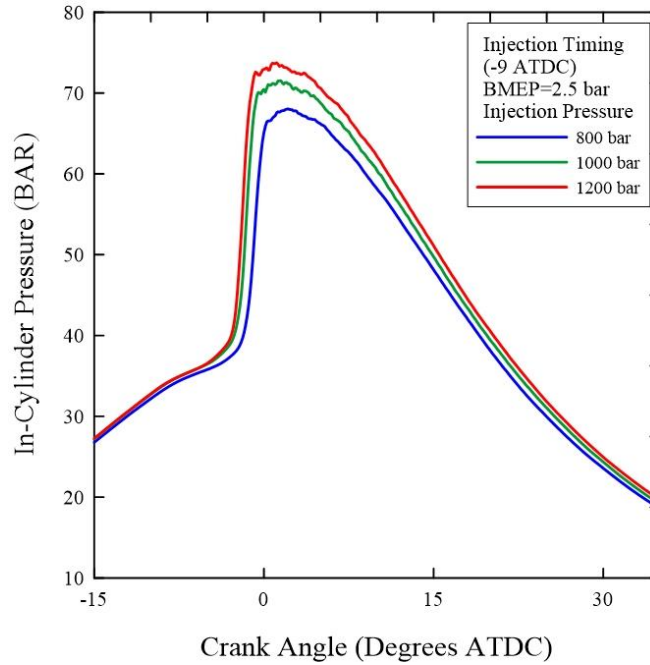


Figure (7) In-cylinder pressure under 40Nm (2.5 bar BMEP) at different injection pressure

In Figure (8) it can be seen that for any injection timing, the higher injection pressure causes a rise of the in-cylinder pressure peak. We also note clearly the decreasing of pressure peaks values when injection timing approaching to TDC and the obvious difference of pressure peaks values at high and low loads. The late injection of fuel in the compression stroke or even at TDC leads to a lower pressure peak due to the occurrence of combustion in the expansion stroke.

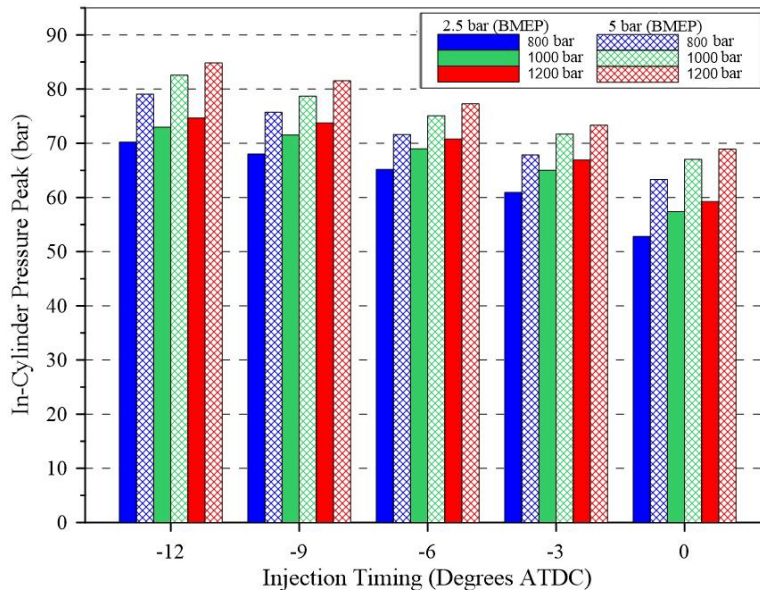


Figure (8) In-cylinder pressure peak at different injection pressure and timing

As a result of increasing the In-cylinder pressure peak with the injection pressure increases, the rate of heat released will increase as shown in figure (9) and figure (10) for high and low loads respectively . In addition, the heat released peak moving forward because earlier starts of combustion.

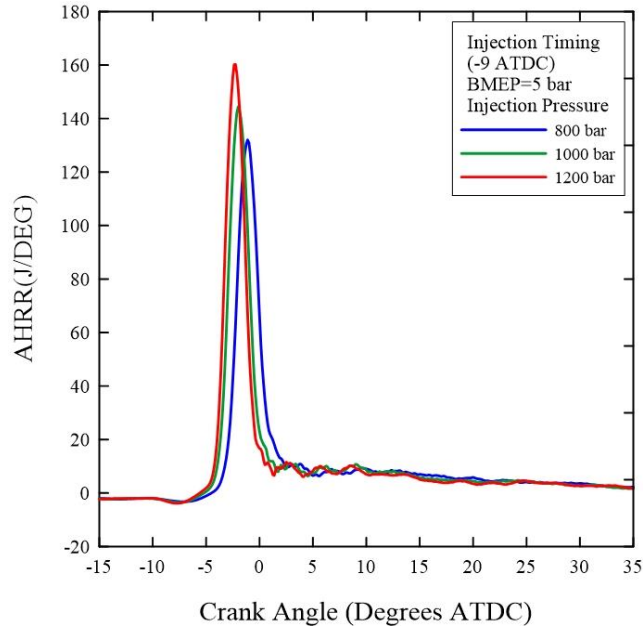


Figure (9) apparent heat release rate under high load at different injection pressure

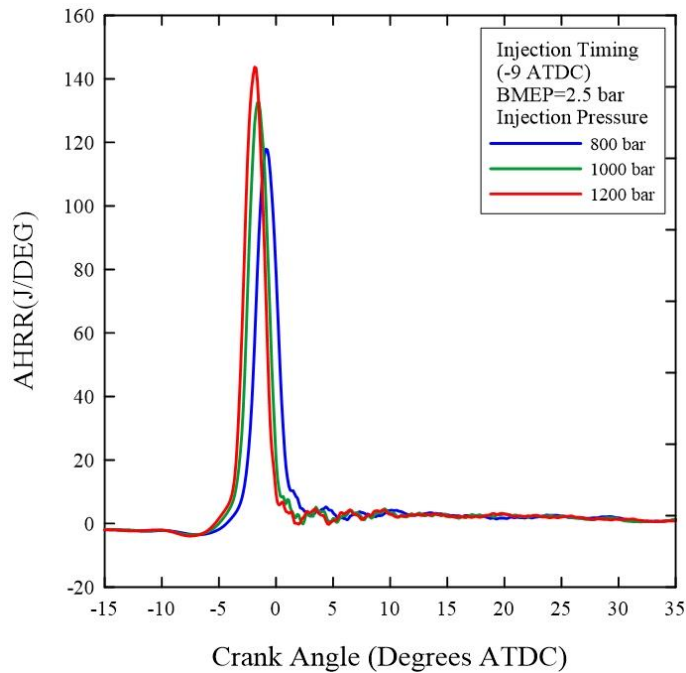


Figure (10) apparent heat release rate under low load at different injection pressure

Figure (11) shows the difference between heat released rate peak at high and low load at different fuel injection pressure. It is observed that AHRR peak for high load is higher than that for low load in all injection timings. This may be because operation temperatures are higher at high load. Vaporization of fuel will occur more readily than at lower temperatures, reducing the physical component of ID time. Therefore, it is probable that the observed reduction in ID at higher load is related to the impact of temperature change upon the physiochemical properties of fuel (its higher viscosity, density, heat capacity, and surface tension, reduced vapor pressure, etc.), which make the fuel generally more resistant to vaporization as shown in figure (12).

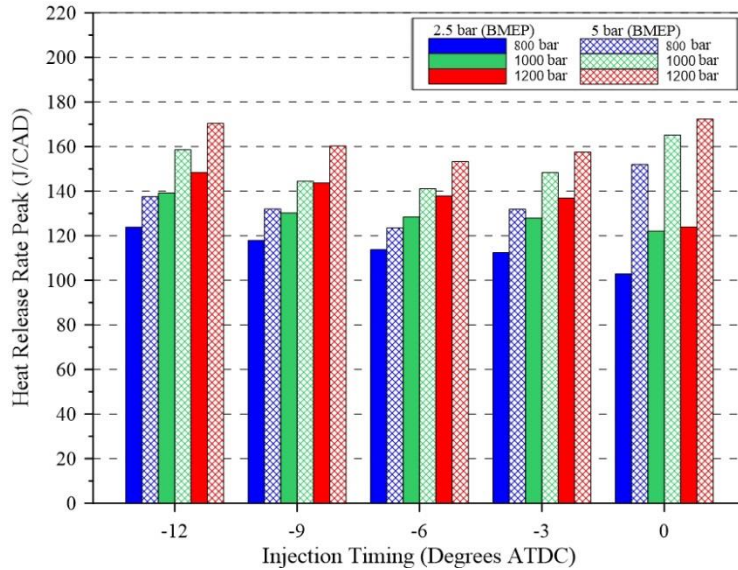


Figure (11) Heat release rate peak under high and low loads at different injection pressure and timing. It can be seen that the ignition delay decreases with an increase in the injection pressure. On average, a reduction of about 1 CAD was observed between 800 bar and 1200 bar for both loads and all injection timings. Higher injection pressure causes better mixing which reduces ignition delay.

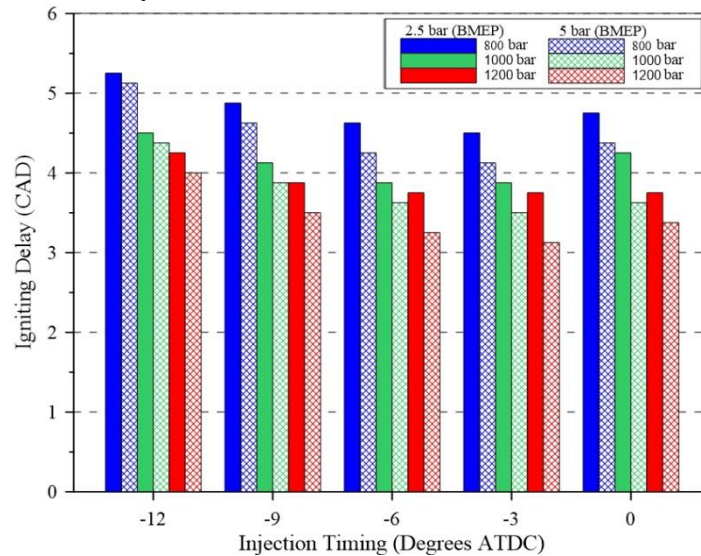


Figure (12) Ignition delay under high and low load at different injection pressure and timing

Besides, it can be noted that the ignition delay at low load was taller than at high load for each injection pressure, because of the relationship between the ignition delay and temperature, as explained above. At late injection (0ATDC) ignition delay again increasing, which leads to an increase premixed burn fraction with a high temperature at high load, the heat released rate peak increase as shown in Figure (11 ).

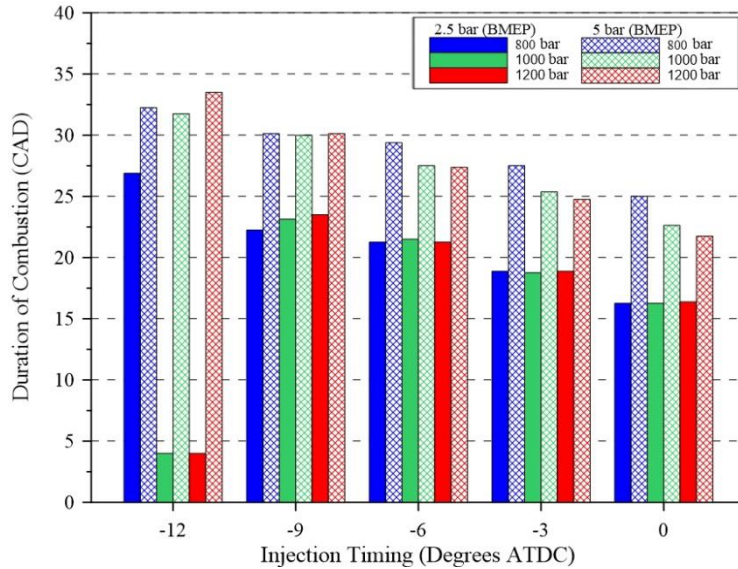


Figure ( 13) effect of injection pressure and timing on duration of combustion

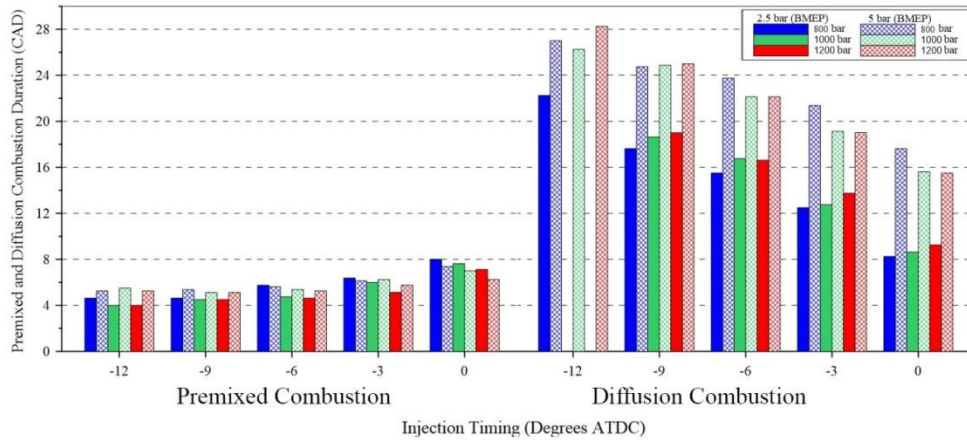


Figure (14) effect of injection pressure and timing on duration of premixed and diffusion combustion

A figure (13, 14) shows the duration of combustion during the premixed and the diffusion combustion phases for different fuel injection pressures. The overall DOC is the sum of premixed and diffusion combustion durations. Within this sum, the change in the

premixed DOC remained almost short, therefore the overall DOC inherits the trend of diffusion combustion duration for all cases. It is noticeable that duration of combustion for high load longer than duration of combustion for low load. In order to understand this, Figure (13) provides information about the duration of combustion in the premixed phase as well as in the diffusion phase. The premixed and diffusion combustion duration are distinguished using the second differential of the heat release rate. There is a significant difference between diffusion combustion duration at high load and diffusion combustion duration at low load, while there are no noticeable differences between the premixed combustion duration at high load and premixed combustion duration at low load. Interestingly, there is no diffusion combustion at conditions of low load, injection timing (-12 ATDC) and injection pressures (1000,1200) bar, This means that the use of high injection pressure at low load with an appropriate injection timing could eliminate the soot. The combustion mode has changed from the Conventional diesel combustion to Homogenous Charge Compression Ignition HCCI by the use of high pressure injection, It is clearly noticeable in fig.(15), Where the diffusion burn fraction was equal to zero

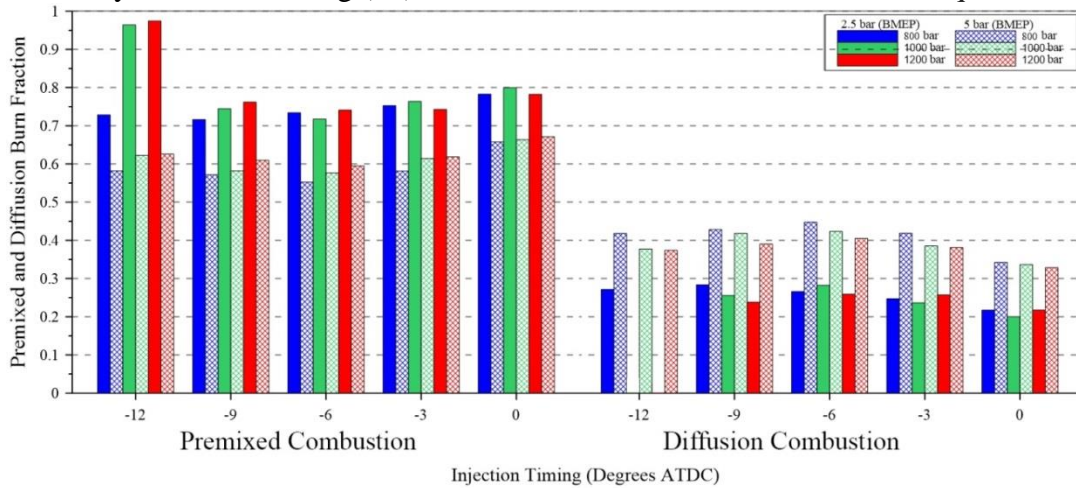


Fig (15) effect of injection pressure and timing on premixed and diffusion burn fraction

In Figure (15) it can be seen that the amount of heat released (burn fraction) during the premixed phase is higher, compared to that of diffusion phase for all injection timings. Generally, the amount of heat released in the premixed combustion phase is strongly connected to the formation of NOx through the correlation of increased in-cylinder combustion temperature. A shorter duration of combustion and lower magnitude of heat released in the premixed phase leads to lower NOx formation. On the other hand, better atomization due to higher injection pressure produces better entrainment, more efficient fuel vaporization and mixture formation. This leads to faster combustion and a higher heat release rate in the premixed phase resulting in a favourable environment of higher in-cylinder temperature and higher NOx emissions. The diffusion phase of combustion is strongly correlated to the soot emission from the engine, thus longer duration of diffusion combustion eventually leads to higher soot formation. The Brake Specific Fuel Consumption (BSFC) for different injection pressure and different injection timings are shown in figure (16). The increase in BSFC at low load is a result of the incomplete combustion of fuel. Therefore, the engine running at low

load is considered uneconomic, Effect of injection timing on fuel consumption was limited.

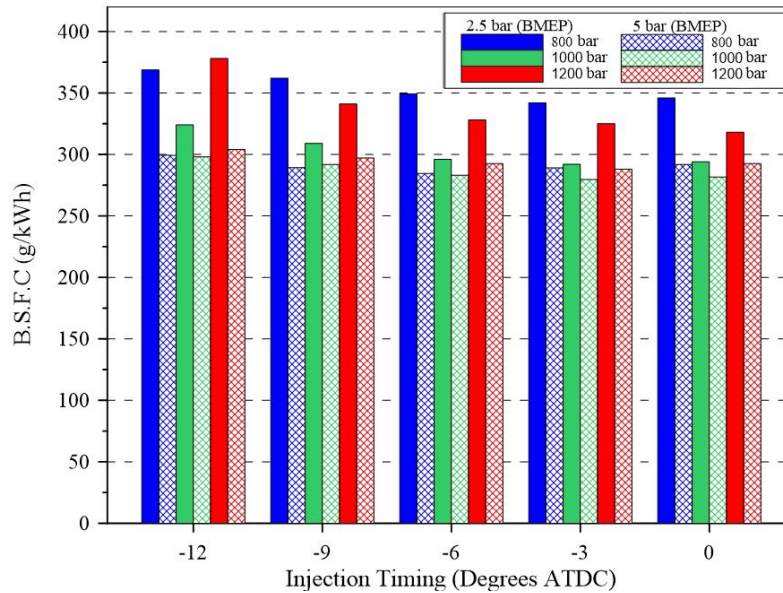


Figure (16) Effect of injection pressure and timing on The Brake Specific Fuel Consumption (BSFC) under high and low load

Increasing the injection pressure has no obvious effect on B.S.F.C at high load , while increasing the injection pressure at low load lead to reduce B.S.F.C .

### 3-2 Emission characteristics

Figure (17) shows the effect of fuel injection pressure at high and low loads with different fuel injection timings, it can be seen that an increase in the fuel injection pressure leads to higher NOx emission. Where the premixed burn fraction increase with injection pressure increasing , which leads to increased heat released and therefore increase the temperature of combustion chamber . The NOx formation during combustion mainly depends on the Zeldowich mechanism where formation reactions are more intensive in a high temperature environment leading to higher NOx emissions. The highest cylinder temperature occurs during the premixed combustion phase where the formation of NOx is dominant. In addition, the retarded injection timing significantly reduces the NOx emissions because of the low in-cylinder temperature resulting from the shift of the combustion into the expansion stroke. As the difference of Nox emissions between high and low-load due to the difference of temperature in combustion chamber.

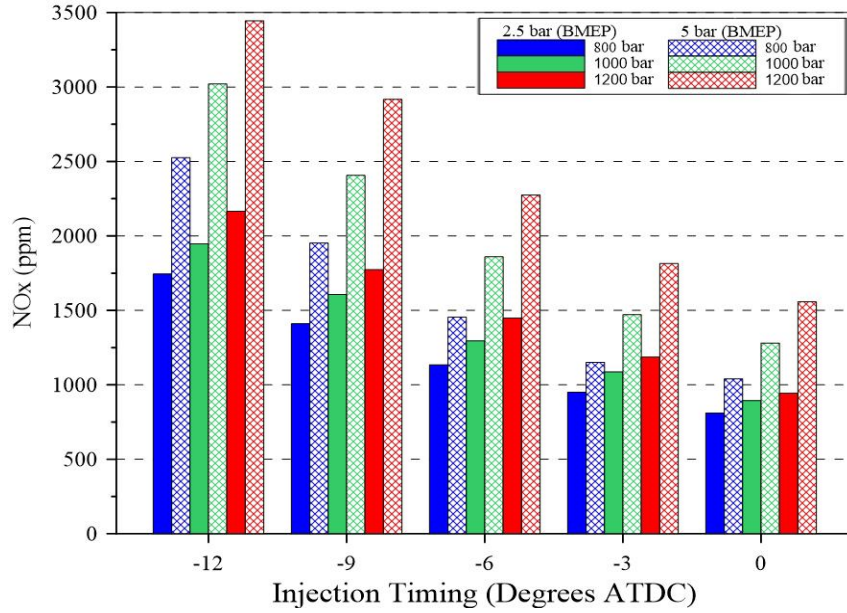


Figure (17) Effect of injection pressure and timing on NOx emissions under high and low load

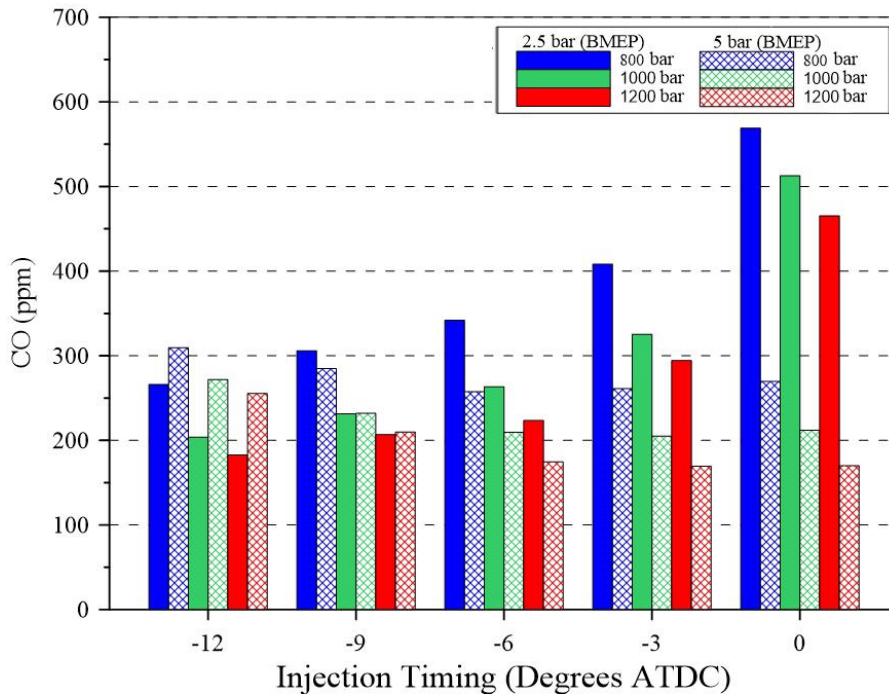


Figure ( 18 ) Effect of injection pressure and timing on carbon monoxide emissions under high and low load

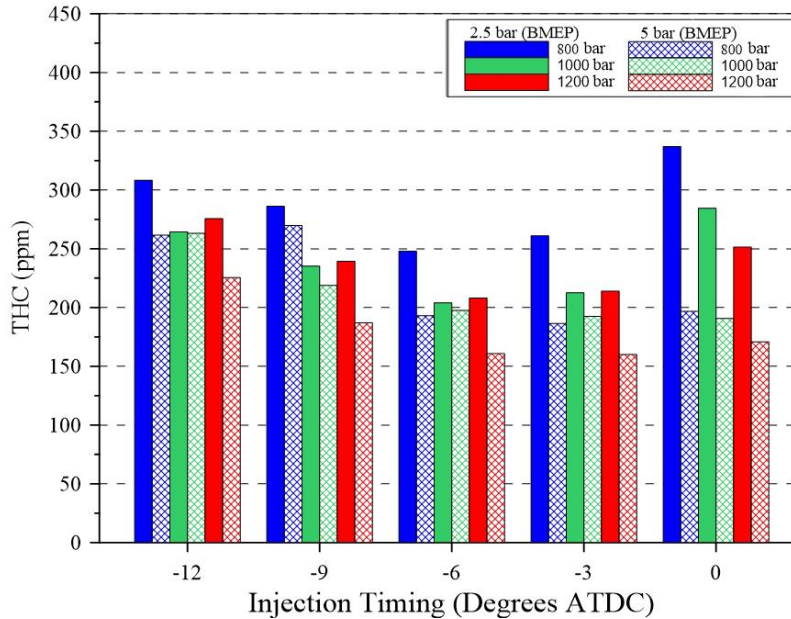


Figure ( 19 ) Effect of injection pressure and timing on (THC) emissions under high and low load

Figures (18) and (19) show the variation of CO and THC emissions at different fuel injection pressures. In figure (18) it can be seen that when fuel injection pressure increases the CO emission decreases. Figure (19) Shows the variation of the THC emissions at different fuel injection pressures. The THC emissions decrease with higher fuel injection pressure. However, the general emission trends for both THC and CO are similar. Both CO and THC emissions are the products of incomplete combustion and they tend to decrease with higher injection pressures. The unburnt hydrocarbon emissions are generally formed as a result of flame quenching. The formation of higher CO and THC emissions are strongly related to the viscosity of fuel. Higher viscosity also leads to longer spray penetration. As a result, wetting of the cylinder walls eventually leads to the formation of higher CO and THC emissions by incomplete combustion.

Figure (20) shows the variations in soot emissions under high and low loads at different injection pressures. The smoke number at all conditions is lowered by increasing the fuel injection pressure. Higher injection pressure leads to the formation of smaller fuel droplets and faster fuel vaporisation due to better entrainment which eventually results in the reduction of smoke emissions. We can clearly note the huge difference in soot emissions between high load and low-load for all timings, This difference results from the large difference in the amount of diffusion combustion (diffusion burn fraction) between high and low-load, as shown in Figure (15). The heat release rate analyses are helpful in understanding NO<sub>x</sub> and soot emissions variations for different conditions. On the other hand, longer duration of the diffusion combustion phase leads to higher soot emissions. Furthermore, retarding the injection timing produces more heat in the premixed phase as shown in figure (15), thus it can be suggested that soot emissions could be lower at late fuel injection timing as shown in figure (20). Late injection led to dramatic change in the mode of combustion as compared with conventional diesel combustion, where late injection lead to semi low temperature combustion (LTC) at high

load and to completely low temperature combustion ( LTC ) at low load where both soot and NOx emissions tend to reduced simultaneously.

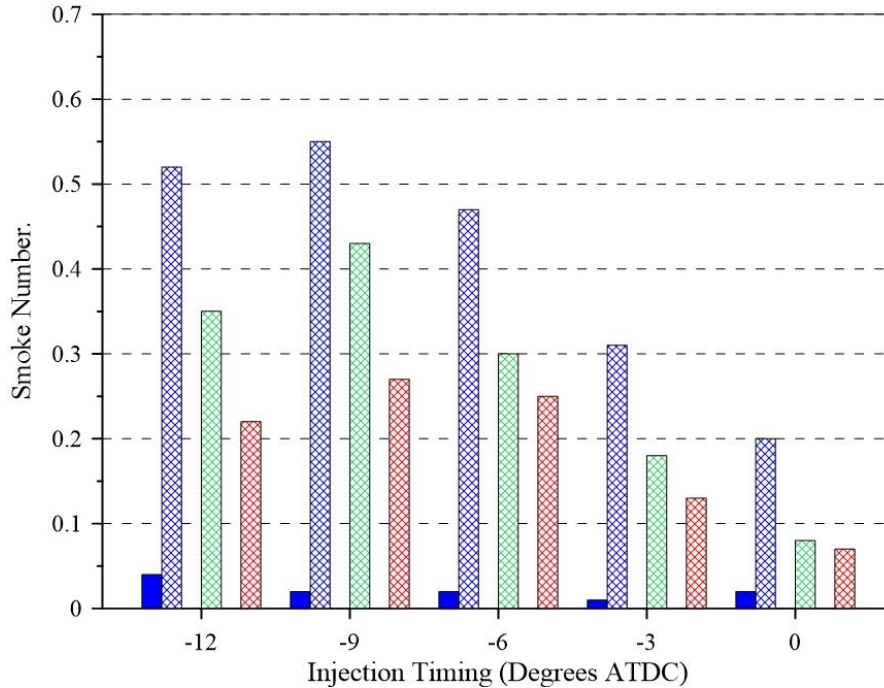


Figure (20 ) Effect of injection pressure and timing on smoke number under high and low load  
Of the most important observations is the lack of a clear emission of soot under low load at fuel injection pressure ( 1000,1200) bar , Due to the fact that the combustion modes at this conditions are (HCC ) at ( injection pressure 1200bar & injection timing -12ATDC ) where the combustion was just premixed combustion as shown in figure ( 15) , and ( PCCI ) & (LTC) at anther conditions .

#### 4- Conclusions

- 1- When the injection pressure was increased, the ignition delay reduced. A shorter ignition delay at high injection pressure also advanced the combustion, and increased the in-cylinder pressure, heat release rate and their peaks respectively.
- 2- The premixed burn fraction increased with fuel injection pressure increasing, this caused a decrease in each of the exhaust SN, THC and CO emissions but the NOx emissions increased.
- 3- At low load with high injection pressure, the combustion mode was changed from conventional diesel combustion to Homogenous Charge Compression Ignition HCCI at advanced injection timing and to ( Premixed Charge Compression PCCI ) & (Low Temperature Combustion LTC ) at late injection timings.
- 4- The diffusion burn fraction at high load is higher than that at low load, which, leads to significant increase of soot emissions compared to those at low load.
- 5- The retardation of the injection timing leads to increase the ignition delay and therefore the premixed burn fraction is larger at late injection conditions, and this explains the characteristics of combustion and emissions at late injection.

## Acknowledgment

The experimental work of this research has been in Centre for Advanced Powertrain and Fuels Research (CAPF), School of Engineering and Design, Brunel University, London, UK

## References

- 1- A.N. Shah, G. Yun-shan, T. Jian-wei, Carbonyls emission comparison of a turbocharged diesel engine fuelled with diesel, biodiesel, and biodiesel-diesel blend, *Jordan Journal of Mechanical and Industrial Engineering* 3 (2) (2009) 111-118.
- 2- A.A. Abdel-Rahman, On the emissions from internal-combustion engines: a review, *International Journal of Energy Research* 22 (1998) 483-513.
- 3- S. Lebedevas, A. Vaicekauskas, Research into the application of biodiesel in the transport sector of Lithuania, *Transport* 21 (2) (2006) 80-87.
- 4- United States Environmental Protection Agency. Fact sheet: diesel exhaust in the United States; 2003. EPA420-F-03-022.
- 5- Council of the European Communities. European Union council directive of 3 December 1987 on the approximation of the laws of the Member States relating to the measures to be taken against the emission of gaseous and particulate pollutants from diesel engines for use in vehicles; 1988. 88/77/EEC.
- 6- Council of the European Communities. Directive 1999/96/EC of the European parliament and of the council of 13 December 1999; 1999. 1999/96/EEC.
- 7- European Parliament and the Council of the European Union. Regulation (EC) No 595/2009 of 18 June 2009; 2009
- 8- DieselNet. <http://www.dieselnets.com/>; 2009.
- 9- US EPA. Summary of current and historical light-duty vehicle emissions standards, [www.epa.gov/greenvehicles/detailedchart.pdf](http://www.epa.gov/greenvehicles/detailedchart.pdf); 2010.
- 10- Suzuki, H., Koike, N., Ishii, H., Odaka, M., 1997. Exhaust Purification of Diesel Engines by Homogeneous Charge with Compression Ignition Part 1: Experimental Investigation of Combustion and Exhaust Emission Behavior Under Pre-Mixed Homogeneous Charge Compression Ignition Method. SAE Paper 970313.
- 11- Suzuki, H., Koike, N., Ishii, H., Odaka, M., 1997. Exhaust Purification of Diesel Engines by Homogeneous Charge with Compression Ignition Part 2: Analysis of Combustion Phenomena and NOx Formation by Numerical Simulation with Experiment. SAE Paper 970315.
- 12- Senda, J., Ikeda, M., Yamamoto, M., Kawaguchi, B., Fujimoto, H., 1999. Low Emission Diesel Combustion System by Use of Reformulated Fuel with liquefied CO<sub>2</sub> and n-Tridecane. SAE Paper 1999-01-1136

- 13- Kawano, D., Senda, J., Kawakami, K., Shimada, A., Fujimoto, H., 2001. Fuel Design Concept for Low Emission in Engine Systems -2nd report Analysis of Combustion Characteristics for the mixed fuels. SAE Paper 2001-01-1071.
- 14- Adomeit, P., Pischinger, S., Becker, M., Rohs, H., Greis, A., Grünefeld, G., 2006. Potential Soot and CO Reduction for HSDI Diesel Combustion Systems. SAE Paper 2006-01-1417.
- 15- Miyamoto, N., Ogawa, H., Nurun, N.M., Obata, K., Arima, T., 1998. Smokeless, Low NO<sub>x</sub>, High Thermal Efficiency, and Low Noise Diesel Combustion with Oxygenated Agents as Main Fuel. SAE Paper 98-05-06.
- 16- Kitamura, T., Ito, T., Senda, J., and Fujimoto, H., 2001. Detailed Chemical Kinetic Modeling of Diesel Spray Combustion with Oxygenated Fuels. SAE Paper 2001-01-1262.
- 17- Xu, Y., Lee, C.F., 2006. Study of Soot Formation of Oxygenated Diesel Fuels Using Forward Illumination Light Extinction (FILE) Technique. SAE Paper 2006-01-1415.
- 18- J.E.Dec. A Conceptual Model of DI Diesel Combustion Based on Laser-Sheet Imaging. SAE, 970873 (1997).
- 19- Majewski, W.A., Khair, M.K., 2006. Diesel Emissions and Their Control. SAE International
- 20- Challen, B. & Baranescu, R. eds., 1999. Diesel Engine Reference Book. Second Edition, Butterworth-Heinemann: Oxford, UK.
- 21- D. M. Peirce, N. S. I. Alozie, D. W. Hatherill, and L. C. Ganippa . Premixed Burn Fraction: Its Relation to the Variation in NO<sub>x</sub> Emissions between Petro- and Biodiesel. Energy Fuels 2013, 27, 3838–3852
- 22- L. Labecki, L.C. Ganippa. Effects of injection parameters and EGR on combustion and emission characteristics of rapeseed oil and its blends in diesel engines. Fuel.2012.03.029
- 23- Rakesh KumarMaurya , DevDattPal , AvinashKumarAgarwal. Digital signal processing of cylinder pressure data for combustion diagnostics of HCCI engine. Mechanical Systems and Signal Processing 36 (2013) 95–109
- 24- S L Kokjohn and R D Reitz. Investigation of charge preparation strategies for controlled premixed charge compression ignition combustion using a variable pressure injection system. International Journal of Engine Research 2010 11: 257
- 25- T Li, M Suzuki and H Ogawa. Effect of Two-Stage Injection on Unburned Hydrocarbon and Carbon Monoxide Emissions in Smokeless Low-Temperature Diesel Combustion with Ultra-High Exhaust Gas Recirculation. International Journal of Engine Research 2010 11: 345
- 26- Zhen Huang, Libin Ji, Dong Han, Zheng Yang and Xingcai Lu. Experimental study on dual-fuel compound homogeneous charge compression ignition combustion. International Journal of Engine Research 2013 14: 23

- 27- Kwanhee Choi, JuwonKim, AhyunKo, Cha-LeeMyung, SimsooPark ,n,Jeongmin Lee . Size-resolved engine exhaust aerosol characteristics in a metal foam particulate filter for GDI light –duty vehicle. *Journal of Aerosol Science* 57 (2013) 1–13
- 28- Sara Pinzi , Paul Rounce , José M. Herreros, Athanasios Tsolakis M. Pilar Dorado. The effect of biodiesel fatty acid composition on combustion and diesel engine exhaust emissions. *Fuel* 104 (2013) 170–182
- 29- Karavalakis, G., Bakeas, E., Stournas, S., 2010. An Experimental Study on the Impact of Biodiesel Origin and Type on the Exhaust Emissions from a Euro 4 Pick-up Truck. SAE Paper 2010-01-2273
- 30- Kawano, D., Mizushima, N., Ishii, H., Goto, Y., Iwasa, K., 2010. Exhaust Emission Characteristics of Commercial Vehicles Fuelled with Biodiesel. SAE Paper 2010-01-2276
- 31- J. Kim , Kwanhee Choi , Cha-Lee Myung , Youngjae Lee , Simsoo Park . Comparative investigation of regulated emissions and nano-particle characteristics of light duty vehicles using various fuels for the FTP-75 and the NEDC mode. *Fuel* 106 (2013) 335–343
- 32- S. Ushakov , Harald Valland , Vilmar Æsøy . Combustion and emissions characteristics of fish oil fuel in a heavy-duty diesel engine. *Energy Conversion and Management* 65 (2013) 228–238
- 33- V. Bermudez , Jose´ M. Lujan, Benjami´n Pla, Waldemar G. Linares. Comparative study of regulated and unregulated gaseous emissions during NEDC in a light-duty diesel engine fuelled with Fischer Tropsch and biodiesel fuels. *bio mass and bioenergy* 35 ( 2011 ) 789-798
- 34- B. Kegl. Influence of biodiesel on engine combustion and emission characteristics. *Applied Energy* 88 (2011) 1803–1812
- 35- Seung Hyun Yoon, Chang Sik Lee. Effect of biofuels combustion on the nanoparticle and emission characteristics of a common-rail DI diesel engine. *Fuel* 90 (2011) 3071–3077.
- 36- M. Mani , G. Nagarajan. Influence of injection timing on performance, emission and combustion characteristics of a DI diesel engine running on waste plastic oil. *Energy* 34 (2009) 1617–1623
- 37- Á Díez, H Zhao, T Carrozzo, A E Catania and E Spessa. Development of a high-speed two-colour system and its application to in-cylinder diesel combustion temperature and soot measurements with split injections. *Proceedings of the Institution of Mechanical Engineers, Part D: Journal of Automobile Engineering* 2012 226: 684
- 38- M. R. Herfatmanesh and Hua Zhao. Experimental investigation of effects of dwell angle on fuel injection and diesel combustion in a high-speed optical CR diesel

- engine. Proceedings of the Institution of Mechanical Engineers, Part D: Journal of Automobile Engineering 2013 227: 246.
- 39- José M Desantes, José M Luján, Benjamín Pla and José A Soler. On the combination of high-pressure and low-pressure exhaust gas recirculation loops for improved fuel economy and reduced emissions in high-speed direct-injection engines. International Journal of Engine Research 2013 14: 3
  - 40- V. Bermúdez , José M. Lujan, Benjamín Pla, Waldemar G. Linares. Effects of low pressure exhaust gas recirculation on regulated and unregulated gaseous emissions during NEDC in a light-duty diesel engine. Energy 36 (2011) 5655-5665.
  - 41- Sarangi, A.K., McTaggart-Cowan, G.P., Garner, C.P., 2010. The Effects of Intake Pressure on High EGR Low Temperature Diesel Engine Combustion. SAE Paper 2010-01-2145.
  - 42- D.C. Rakopoulos. Heat release analysis of combustion in heavy-duty turbocharged diesel engine operating on blends of diesel fuel with cottonseed or sunflower oils and their bio-diesel. Fuel 96 (201 2) 524–534
  - 43- S. Manasra, D. Brueggemann. Effect of Injection Pressure and Timing on the In-Cylinder Soot Formation Characteristics of Low CR Neat GTL-Fueled DI Diesel Engine. SAE Paper 2011-01-2464
  - 44- C. Sayin , M. Gumus. Impact of compression ratio and injection parameters on the performance and emissions of a DI diesel engine fueled with biodiesel-blended diesel fuel. Applied Thermal Engineering 31 (2011) 3182-3188.
  - 45- S. Puhan, R. Jegan, K. Balasubbramanian, G. Nagarajan, Effect of injection pressure on performance, emissions, and combustion characteristics of high linolenic linseed oil methyl ester in a DI diesel engine, Renewable Energy 34(2009) 1227-1233.
  - 46- Heywood, J.B., 1988. Internal Combustion Engine Fundamentals McGraw-Hill Science Engineering.